

Viscosity effects on optically generated electron and nuclear spin hyperpolarization

Electronic Supplementary Information (ESI)

Matthew W. Dale,^a Daniel J. Cheney,^b Claudio Vallotto,^a and Christopher J. Wedge^{*a,b}

Contents

Experimental details	2
Materials	2
Sample Concentrations	2
Sample Conditions	2
Transient Absorption	2
Kinetic Parameters	3
Table S1 Rate constants for different volume fractions of glycerol	3
Additional Data	4
Figure S1 Oxygen and radical effects on DAF-EPR	4
Table S2 Electronic polarization for different nitroxide radicals	4
Figure S2 Laser power dependence of DAF-EPR	5
Figure S3 Optical DNP enhancements with 1.0 W illumination	5
References	6

Experimental details

Materials

Rose Bengal (Aldrich 95%), TEMPO (Aldrich 98%), 4-hydroxy-TEMPO (Aldrich 97%), 4-amino-TEMPO (Aldrich 97%), glycerol (BioUltra $\geq 99.5\%$), Sodium phosphate monobasic dihydrate (purum p.a. $\geq 99.0\%$), and Sodium phosphate dibasic (BioXtra $\geq 99.0\%$), were purchased from Sigma-Aldrich and used without further purification. Milli-Q water (resistivity 18.2 M Ω cm) was produced on site.

Sample Concentrations

Sample concentrations were verified by UV-visible spectroscopy using a Perkin Elmer Lambda 1050 spectrophotometer. The extinction coefficient of rose bengal at 532 nm was determined to be $5.6 \times 10^4 \text{ M}^{-1} \text{ cm}^{-1}$ and used to verify consistency of dye concentration between samples.

The extinction coefficient of TEMPOL in water at 429 nm ($13.4 \text{ M}^{-1} \text{ cm}^{-1}$) was used to prepare a radical standard to which subsequent radical stock solutions could be conveniently compared by double integration of their CW-EPR spectra.¹ These additional CW-EPR measurements were performed using a Bruker EMX spectrometer using a high-sensitivity cylindrical mode cavity (ER 4119HS), with samples contained in 1 mm i.d. tubes (Wilma 712-SQ).

Sample Conditions

With the exception of the preliminary experiment shown in Fig. S1a all samples were deoxygenated by nitrogen bubbling for 20 minutes before analysis. Whereas the acidity of water can be lowered by dissolved CO₂ leading to a pH of around 5.7,² nitrogen bubbling also removes this gas giving a neutral sample pH even in the absence of pH buffer. The sample flow and nitrogen bubbling also act to continuously mix our solution, acting to prevent the sort of nanophase separation of glycerol-water solutions reported to effect solid-state DNP studies after sample vitrification.³ To prevent diffusion of atmospheric gases back into the sample through the PTFE sample tubing during the experiment a constant nitrogen gas flow through an outer jacket around the tube is used. As described previously this constant purge of gas into the resonator also acts to prevent sample heating.⁴

The time averaged laser power in pulsed EPR measurements is at most 120 mW which is insufficient to cause any significant sample heating, whereas the continuous-wave laser source operating at up to 2.0 W in the NMR measurements can produce a measurable increase in sample temperature. While direct measurements of the sample temperature are difficult we previously estimated the increase in temperature upon illumination using the variation in the nuclear relaxation time, T_{1n} , in a sample without the radical. This showed an increase in temperature of less than 10 K under continuous illumination with a divergent 1.0 W laser diode at 520 nm.⁴ While a more powerful 532 nm laser source is used in the present study the collimated beam has allowed introduction of a beam shutter to gate the illumination in order to reduce heating effects despite the higher source power. This gating prevents an accurate NMR measurement of sample temperature as the inversion recovery timescale is comparable to or longer than the illumination periods used. Measurement of temperature based on the chemical shift of water is also precluded in our low field experiment due to insufficient chemical shift resolution to measure the 0.010 ppm K⁻¹ shift expected.⁵

Transient Absorption

Transient absorption spectroscopy was carried out using home built apparatus with pulsed excitation (355 nm, 9.0 mJ per pulse at 20 Hz) from a frequency doubled Nd:YAG laser (Continuum Surelite SL I-20 Hz) incident perpendicular to a continuous probe beam at 633 nm from a HeNe laser (Uniphase 1101). Samples were contained within a 5 mm \times 5 mm optical path-length cuvette (Hellma 111-057-QS). The probe beam was focussed onto an amplified Si detector (Thorlabs PDA10A-EC) with long pass filter (Thorlabs FEL600) to remove excitation and fluorescence signals, and transients digitized using a 16-bit oscilloscope (PicoScope 5244A) triggered synchronously with the excitation laser Q-switch.

^a Department of Physics, University of Warwick, Gibbet Hill Road, Coventry, CV4 7AL, UK.

^b Department of Chemical Sciences, University of Huddersfield, Huddersfield, HD1 3DH, UK.

^{*} Current Affiliation: University of Huddersfield, E-mail: c.wedge@hud.ac.uk

Kinetic Parameters

Initial attempts to fit TR-EPR data considered only those processes shown in equations 1–5, with Stern-Volmer analysis of transient absorption data providing values of $k_q = (2.01 \pm 0.02) \times 10^9 \text{ M}^{-1} \text{ s}^{-1}$ and $k_d = (4.9 \pm 0.1) \times 10^5 \text{ s}^{-1}$ in phosphate buffered solution in agreement with those of Takahashi *et al.*⁶ As shown in Fig. S1a the transient magnetization is increased by removal of oxygen, hence kinetic parameters were redetermined under deoxygenated conditions obtaining $k_q = (1.7 \pm 0.1) \times 10^9 \text{ M}^{-1} \text{ s}^{-1}$ and $k_d = (1.2 \pm 0.8) \times 10^5 \text{ s}^{-1}$.

The triplet-triplet annihilation rate k_{tt} is more difficult to measure so in previous studies of RTPM polarization of Rose Bengal was assumed to occur at a diffusion controlled rate of $7.4 \times 10^9 \text{ M}^{-2} \text{ s}^{-1}$. Such a rate readily derived from the Einstein-Smoluchowski equation is appropriate for uncharged species but given the dianionic nature of Rose Bengal a correction should be made which decreases the rate by a factor of ~ 0.45 (depending on solvent permittivity) due to repulsion between the similarly charged species.^{7,8} In preliminary work considering only the processes shown in equations 1–5 we found empirically that an even lower rate of $8 \times 10^8 \text{ M}^{-2} \text{ s}^{-1}$ is necessary to produce a global fit to our experimental data. This is in fact in good agreement with the value of $7.8 \times 10^8 \text{ M}^{-2} \text{ s}^{-1}$ reported by Ludvíková *et al.* in a detailed study of the photochemistry of Rose Bengal in aqueous solution.⁹ This study also included additional photochemical processes given by equations 6–9. Our final fitting routine includes these additional processes affecting the concentration of the triplet dye molecule, with equations 10–13 solved numerically. The kinetic parameters obtained independently by Ludvíková *et al.* are used with the exception of the radical quenching rate k_q which was not considered in this report and hence the value of $1.7 \times 10^9 \text{ M}^{-1} \text{ s}^{-1}$ from our Stern-Volmer analysis is used.

To fit data in glycerol containing solutions it is necessary to scale the rate constants for the various photochemical processes. While k_d and k_q would be amenable to simple measurement through further transient absorption experiments this is not the case for the other rate constants, hence for consistency all kinetic parameters were scaled according to the variation in solution viscosity with the values used as indicated in Table S1. Note that for second order processes the correct scaling factor is the square of the viscosity ratio.⁸

Table S1 Kinetic parameters used in simulation of TR-EPR data. Those for samples with added glycerol are determined by scaling using the viscosity ratio. Translational diffusion constants are also given for reference.

Volume fraction glycerol / %	0	10	20	30
Viscosity ^a / mPa·s	0.981	1.35	1.93	2.91
D_r , Rose Bengal / $10^{-10} \text{ m}^2 \text{ s}^{-1}$	2.1 ^b	1.5	1.1	0.7
D_r , TEMPO / $10^{-10} \text{ m}^2 \text{ s}^{-1}$	4.1 ^c	3.0	2.1	1.4
$k_d / 10^4 \text{ s}^{-1}$	2.14 ^d	1.56	7.90	2.66
$k_{tt} / 10^8 \text{ M}^{-1} \text{ s}^{-1}$	7.79 ^d	5.66	2.88	0.97
$k_q / 10^8 \text{ M}^{-1} \text{ s}^{-1}$	8.95 ^e	4.73	1.22	1.38
$k_{sq} / 10^8 \text{ M}^{-1} \text{ s}^{-1}$	5.37 ^d	2.84	0.731	0.0831
$k_{\text{redox}^*} / 10^7 \text{ M}^{-1} \text{ s}^{-1}$	5.39 ^d	2.85	0.734	0.268
$k_{\text{redox}^{**}} / 10^8 \text{ M}^{-1} \text{ s}^{-1}$	1.73 ^d	0.914	0.236	0.0268
$k_{\text{bet}} / 10^9 \text{ M}^{-1} \text{ s}^{-1}$	4.72 ^d	2.50	0.643	0.073

^a A variety of different dynamic viscosity values of glycerol water mixtures are reported in the literature. Those given here are appropriate for a solution at 294 K, according to a numerical model for glycerol-water mixtures,^{10,11} ^b from ref. 12, ^c from ref. 13, ^d from ref. 9, ^e from fitting of TR-EPR data for a de-oxygenated sample without pH buffer.

Additional Data

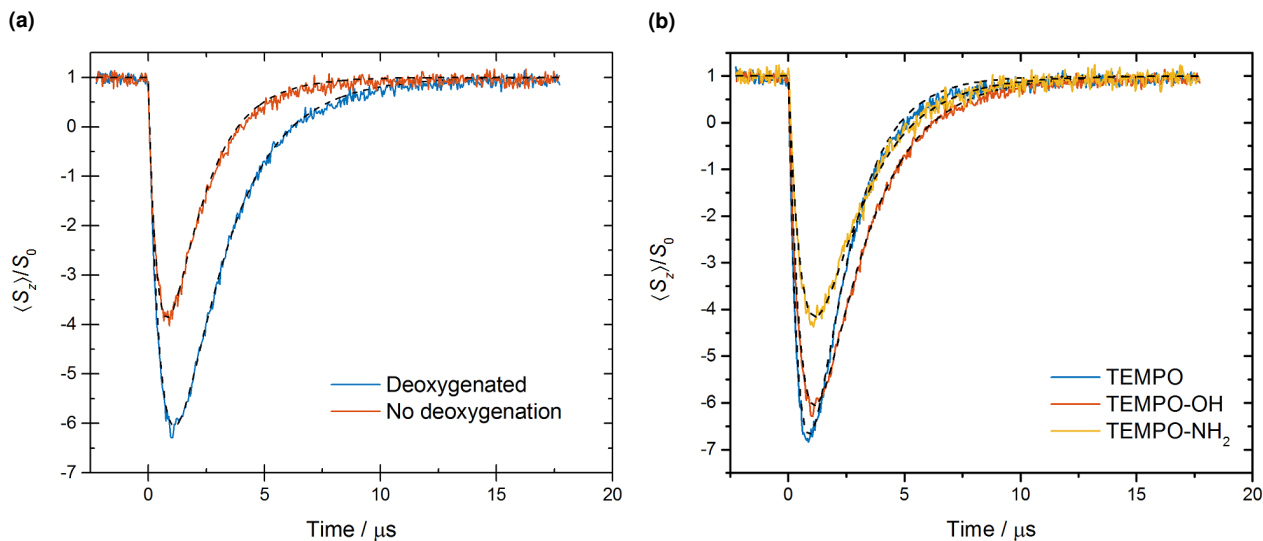


Fig. S1 Delay after flash (DAF) EPR experiments for aqueous solutions of Rose Bengal (0.2 mM) and nitroxide radical (0.2 mM) a) for TEMPO with and without deoxygenation by nitrogen bubbling and b) for deoxygenated samples of three different radical variants as indicated. In each case the dashed line is a numerical fit to the experimental data. To fit the data for the sample without deoxygenation the shorter experimentally determined T_{1e} of 453 ns vs 683 ns was used and the triplet decay rate k_d allowed to increase, while holding other kinetic parameters constant. The profiles for different radicals were fitted using experimentally determined T_{1e} values and allowing only the polarization P_{net} to vary (Table S2). Illumination is 6 mJ/pulse at 532 nm, with the lower magnitude of the peak magnetization in these data sets compared to those presented elsewhere due to differences in the laser focus leading to lower pulse energy at the sample.

Table S2 Effect of varying the identity of the radical on the RTPM polarization P_{net} in deoxygenated solutions of Rose Bengal, along with peak transient magnetization values for 6 mJ/pulse illumination and measured electronic relaxation time. Polarization values are given relative to the TEMPO case. Rose Bengal and radical concentrations both 0.2 mM

Radical	P_{net} (normalised)	$\langle S_z \rangle_{max} / S_0$	T_{1e} / ns
TEMPO	1.00	-6.6	520
TEMPO-OH	0.81	-6.4	680
TEMPO-NH ₂	0.59	-4.4	670

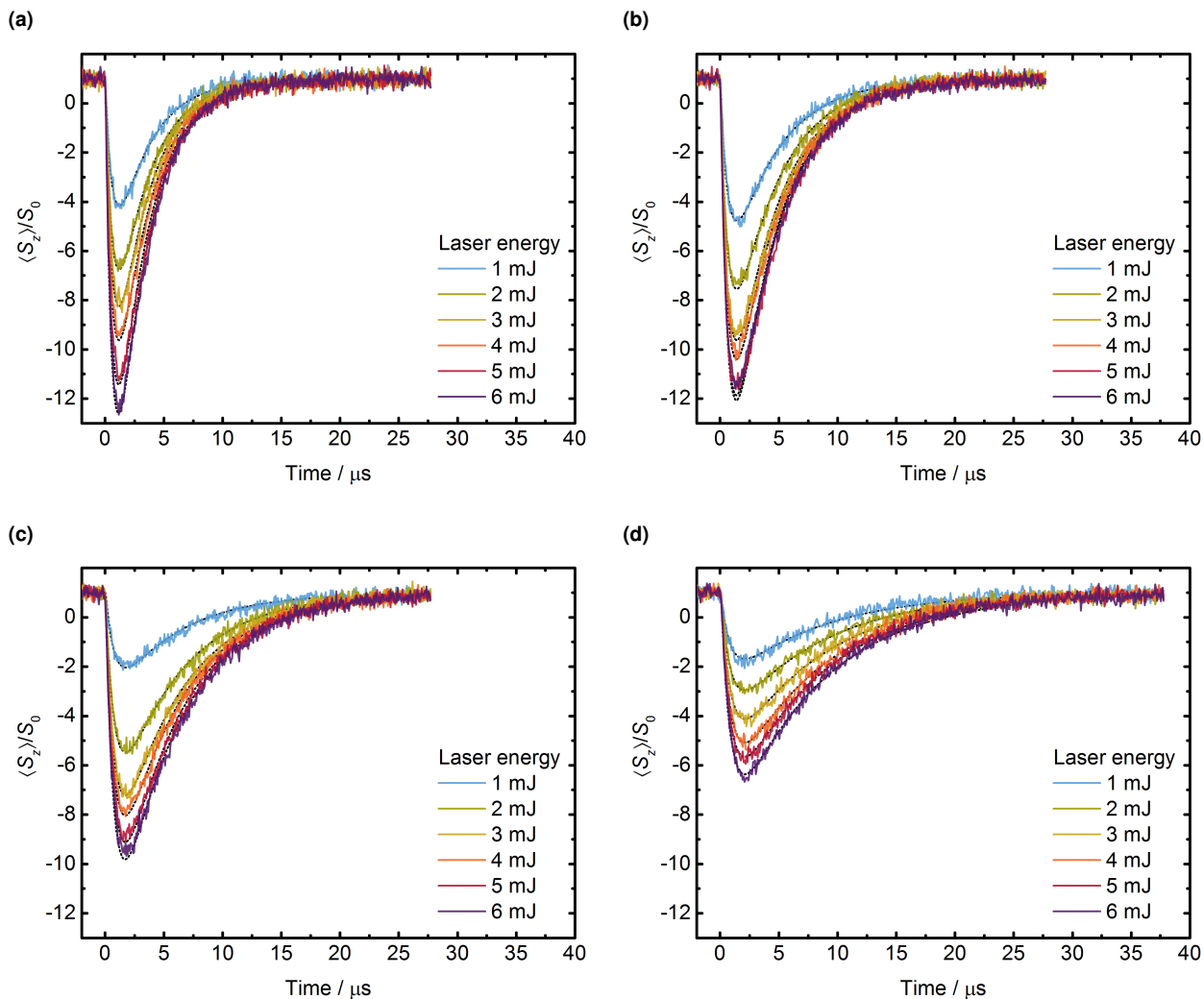


Fig. S2 Delay after flash EPR experiments for deoxygenated aqueous solutions of Rose Bengal (0.2 mM) and TEMPO (0.2 mM) for different solution conditions a) in the absence of glycerol or with b) 10%, c) 20%, d) 30% added glycerol by volume. All solutions were deoxygenated by nitrogen bubbling and photoexcited at 532 nm with average laser pulse energies as indicated. In each case the dashed line is a numerical fit to the experimental data. Rate constants used in the fits are as indicated in Table S1, with measured T_{1e} values and relative polarization determined from these fits indicated in Table 1. We note that an alternative fitting regime assuming P_{net} to be invariant on glycerol addition and allowing the initial triplet concentration to vary was trialed and could not adequately reproduce these data sets.

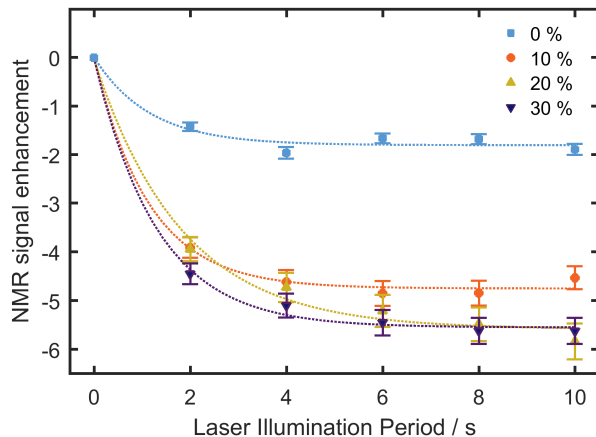


Fig. S3 Optically generated enhancement in ^1H NMR signal intensity with varying illumination time at a power of 1.0 W for volume fraction of glycerol as indicated. Dotted lines show monoexponential fits to the data as a guide to the eye.

References

- 1 D. Barr, J. Jiang and R. T. Weber, *How to Quantitate Nitroxide Spin Adducts Using TEMPOL*, EPR Experimental Techniques, Bruker Instruments, Inc., EPR Division, Billerica, MA, 01821 USA, 2001, vol. 3.
- 2 H. T. Byck, *Science*, 1932, **75**, 224–224.
- 3 E. M. M. Weber, G. Sicoli, H. Vezin, G. Frébourg, D. Abergel, G. Bodenhausen and D. Kurzbach, *Angew. Chem. Int. Ed.*, 2018, **57**, 5171–5175.
- 4 M. W. Dale and C. J. Wedge, *Chem. Commun.*, 2016, **52**, 13221–13224.
- 5 A. Hartel, P. Lankhorst and C. Altona, *Eur. J. Biochem.*, 1982, **129**, 343.
- 6 H. Takahashi, M. Iwama, N. Akai, K. Shibuya and A. Kawai, *Mol. Phys.*, 2014, **112**, 1012–1020.
- 7 F. Morel and J. G. Hering, *Principles and applications of aquatic chemistry*, Wiley, New York Chichester, 1993.
- 8 M. J. Pilling and P. W. Seakins, *Reaction kinetics*, Oxford University Press, Oxford, 1997.
- 9 L. Ludvíková, P. Friš, D. Heger, P. Šebej, J. Wirz and P. Klán, *Phys. Chem. Chem. Phys.*, 2016, **18**, 16266–16273.
- 10 N.-S. Cheng, *Ind. Eng. Chem. Res.*, 2008, **47**, 3285–3288.
- 11 C. Westbrook, *Calculator to estimate the density and viscosity of glycerine / water mixtures*, 2017, http://www.met.reading.ac.uk/~sws04cdw/viscosity_calc.html.
- 12 T. Kakiuchi and Y. Takasu, *J. Phys. Chem. B*, 1997, **101**, 5963–5968.
- 13 P. J. van Bentum, G. H. van der Heijden, J. A. Villanueva-Garibay and A. P. Kentgens, *Phys. Chem. Chem. Phys.*, 2011, **13**, 17831–40.